1 **THE PARALLEL AUDITORY BRAINSTEM RESPONSE**

2

3 Melissa J Polonenko, Ph.D. (ORCID: 0000-0003-1914-6117)

4 Ross K Maddox, Ph.D.* (ORCID: 0000-0003-2668-0238)

5

6 Department of Biomedical Engineering
7 Department of Neuroscience
8 Del Monte Institute for Neuroscience
9 University of Rochester

10

11 *correspondence:
12 University of Rochester
13 Goergen Hall
14 Box 270168
15 Rochester, NY 14627

16 Email: ross.maddox@rochester.edu

ABSTRACT

The frequency-specific tone-evoked auditory brainstem response (ABR) is an indispensable tool in both the audiology clinic and research laboratory. Most frequently the toneburst ABR is used to estimate hearing thresholds in infants, toddlers and other patients for whom behavioral testing is not feasible. Therefore, results of the ABR exam form the basis for decisions regarding interventions and hearing habilitation with implications extending far into the child's future. Currently, responses are elicited by periodic sequences of toneburst stimuli presented serially to one ear at a time, which take a long time to measure multiple frequencies and intensities, and provide incomplete information if the infant wakes up early. Here we describe a new method, the parallel ABR (pABR), which uses randomly timed toneburst stimuli to simultaneously acquire ABR waveforms to 5 frequencies in both ears. Here we describe the pABR and quantify its effectiveness in addressing the greatest drawback of current methods: test duration. We show that in adults with normal hearing the pABR yields high-quality waveforms over a range of intensities, with similar morphology to the standard ABR in a fraction of the recording time. Furthermore, longer latencies and smaller amplitudes for low frequencies at a high intensity evoked by the pABR versus serial ABR suggest that responses may have better place specificity due to the masking provided by the other simultaneous toneburst sequences. Thus, the pABR has substantial potential for facilitating faster accumulation of more diagnostic information that is important for timely identification and treatment of hearing loss.

KEYWORDS

auditory brainstem response, evoked potentials, objective audiometry, electroencephalography, assessment

INTRODUCTION

The frequency-specific auditory brainstem response (ABR) is an essential diagnostic tool for estimating audiometric thresholds in infants and other patients for whom behavioral thresholds are difficult or impossible to obtain. Accurate threshold estimation is critical to determining the need for auditory prostheses such as hearing aids or cochlear implants, and for enrollment in appropriate habilitation programs. This process needs to occur quickly because earlier intervention promotes better spoken speech and language outcomes in children (Ching et al., 2014; Cullington et al., 2017; Harrison, Gordon, & Mount, 2005; Joint Committee on Infant Hearing, 2007; May-Mederake, 2012; Moeller, 2000; Yoshinaga-Itano, Sedey, Coulter, & Mehl, 1998). The toneburst ABR has been the gold-standard for infant assessment because testing can be completed while the infant sleeps and its thresholds highly correlate (up to 0.9) with behavioral thresholds when a large range of thresholds is considered (Gorga et al., 2006; Ramos, Almeida, & Lewis, 2013; Stapells & Oates, 1997). While effective at estimating hearing thresholds, the diagnostic ABR suffers from an important constraint: test time. We aim to describe and validate the feasibility of our new parallel ABR (pABR) method which is designed to address this time constraint by presenting multiple frequencies in both ears simultaneously.

Reducing test time is important for two main reasons. A diagnostic ABR exam entails measuring a series of individual responses at several frequencies over a range of intensities in both ears (American Academy of Audiology, 2012; Hood, 1998, p. 98; Hyde, 2008). Because the exam is highly sensitive to movement artifacts, the ABR is typically performed while the infant sleeps. This constrains the duration of the test to that of the infant's nap, which also makes the endpoint unpredictable. To compensate, audiologists must make decisions about which frequencies and intensities are the most important to acquire in which ears and pursue those first (e.g., BC Early Hearing Program, 2012, p. 18). If the infant wakes up earlier than anticipated, the audiologist is forced to choose between inferring thresholds from incomplete data or scheduling a return visit in which the test can be completed. This delays diagnosis and treatment, poses risks for attrition, carries additional costs, and adds stress to the family as they await clinical decisions. This is not a trivial burden of time: approximately 150,000 infants are referred for the exam each year in the United States alone, with about 10,000 found to be deaf or hard-of-hearing (Task Force on Newborn and Infant Hearing, 1999; Vohr, 2003). Reducing the exam time and the need for additional visits will free up clinician time and resources, lowering the barrier for referral and increasing the likelihood that children receive the needed care in a timely manner. Accurate threshold estimates must be obtained—early intervention in patients with elevated thresholds leads to improved language, cognitive, and educational outcomes later in childhood.

The second reason test times need to be shortened is to minimize exposure to sedation and anesthesia. While newborns are able to sleep during the exam, infants over four months old and young children often cannot sit still or sleep, requiring the use of sedation or general anesthesia (François, Teissier, Barthod, & Nasra, 2012; Hood, 1998, p. 122). Recent studies investigating the effects of anesthesia on the developing brain suggest a risk of neurotoxicity. Even a few hours of exposure can result in significant neuronal loss in young animals, with deleterious effects persisting later in life (Wagner, Ryu, Smith, & Mintz, 2014; Jevtovic-Todorovic et al., 2003; Creeley et al., 2013; Brambrink et al., 2012). In children, the risk of learning disabilities increases with longer accumulated exposure to some drugs (Wilder et al., 2009). Based on these findings, the FDA issued a warning that general anesthesia and sedation drug use should be avoided or minimized wherever possible for children under three years of age, and should be limited to three cumulative hours (FDA, 2017). Diagnostic ABRs routinely last between 1 to 3 hours, using up the recommended exposure times for the first three years of life. Shortening the diagnostic ABR exam would reduce dosages, and in some situations may make it possible to run the test without drugs. Thus, the imperative to reduce test time extends beyond cost and convenience: it is essential for reducing the risk of damaging the developing brain.

The signal-to-noise ratio (SNR) of an ABR measurement principally drives how long the measurement takes because an ABR waveform is the averaged responses to several thousand repetitions of a stimulus. The SNR of the averaged waveform improves as the number of stimulus repetitions increases. Thus, an attractive way to attempt shortening test time involves increasing the rate at which stimuli are presented. Increasing the stimulus rate in practice, however, carries important drawbacks. With typical periodic stimulus presentation, the time window in which the ABR waveform can be viewed is limited to the inter-stimulus period, or the inverse of the stimulus rate. Relevant ABR components can have latencies of 12–15 ms, which practically limits the rate to 70–80 Hz. Several studies have sidestepped this constraint by

95 replacing periodic stimulus timing with various types of jitter or randomization schemes, allowing
96 stimulation rates into the high hundreds of hertz or beyond (Eysholdt & Schreiner, 1982; Özdamar &
97 Bohórquez, 2006; Valderrama et al., 2012, 2014; Wang, Zhan, Yan, Bohórquez, & Özdamar, 2013). These
98 high rates reduce noise, but neural adaptation shrinks responses (i.e., signal), which in turn partially or
99 completely cancels out SNR gains that the faster rates might have provided. Timing randomization shows
100 some benefit at rates in the low hundreds of stimuli per second, but a lack of translation to the clinic
101 suggests those are outweighed by the increased complexity of analysis and a lack of normative data.
102 Additionally, these studies have focused on clicks, rather than more diagnostically relevant toneburst
103 stimuli.

104 Recording time could also be reduced if responses to different frequency bands could be recorded
105 simultaneously. This is the approach taken by the multiple auditory steady-state response (ASSR). A single
106 ASSR stimulus is constructed by modulating a sinusoid carrier at the audiometric test frequency. Rather
107 than the waveform, the response is a single automatically derived number (e.g., an F-test) that quantifies
108 the neural phase-locking to the modulator. Giving each test frequency an independent modulation rate
109 allows separate assessment of responses to several simultaneously presented stimuli. The ASSR can
110 effectively reduce test time and estimate thresholds that correlate with behavioral thresholds (Luts,
111 Desloovere, & Wouters, 2006), but it also carries drawbacks. The ASSR does not provide the response
112 waveforms that audiologists are experts in interpreting. The way the stimuli are constructed also leads to
113 much higher energy than equivalent toneburst stimuli, which means the clinician must be careful not to
114 expose the patient to potentially dangerous levels. Despite its availability in a number of clinical devices,
115 the ASSR has seen narrower adoption than the frequency-specific ABR as a diagnostic exam in the clinic.

116 The goal of this paper is to provide proof of principle for a new paradigm for measuring the ABR to all
117 frequencies in both ears in parallel. The parallel pABR is accomplished through designing stimuli
118 comprised of simultaneous, independently randomized sequences of toneburst stimuli. First, we validate
119 that the paradigm yields high quality canonical brainstem responses at stimulus levels ranging from high to
120 very low, suggesting the pABR's utility for estimating audiometric thresholds. These responses exhibit
121 standard ABR morphology, minimizing the need for clinician retraining. We then show that the time to
122 reach a satisfactory SNR and residual noise value is better for parallel presentation than for the same
123 randomized toneburst trains presented in serial, especially at lower intensities. Taken together, these
124 findings demonstrate the pABR's feasibility to meaningfully reduce diagnostic test time with few drawbacks.

125

METHODS

Human subjects

128 Experiments were completed using a protocol approved by the University of Rochester Research Subjects
129 Review Board (#66988). All subjects gave informed consent prior to participation and were compensated
130 for their time. We collected data from 10 subjects (5 females) with a mean ± SD age of 22.6 ± 4.6 years
131 (range: 18.3 to 34.2 years old). Pure-tone audiometric screening confirmed normal hearing thresholds
132 (≤ 20 dB HL) for each subject at octave frequencies between 500 and 8000 Hz. Subjects self-reported no
133 other neurological abnormalities.

134

Stimulus construction

136 Figure 1 depicts stimulus construction for the pABR. As an overview (details given in the next sections),
137 pABR stimuli are constructed from windowed tonebursts centered at octave frequencies from 500 Hz to
138 8000 Hz. For each frequency, a toneburst train is created by placing tonebursts randomly within a 1 s
139 epoch. This is repeated for all other frequencies with independent random processes controlling the timing.
140 All toneburst trains are summed, and the process repeated with new random processes for the other ear,
141 comprising a stimulus epoch. Because of the independent timing, we can separately compute the average
142 ABR waveform to each toneburst train from the same electroencephalography (EEG) data free from
143 interference. The stimulus presentation rate and intensity can be varied, and we can compare pABR
144 acquisition to single-frequency serial acquisition by presenting all or only one of the toneburst trains,
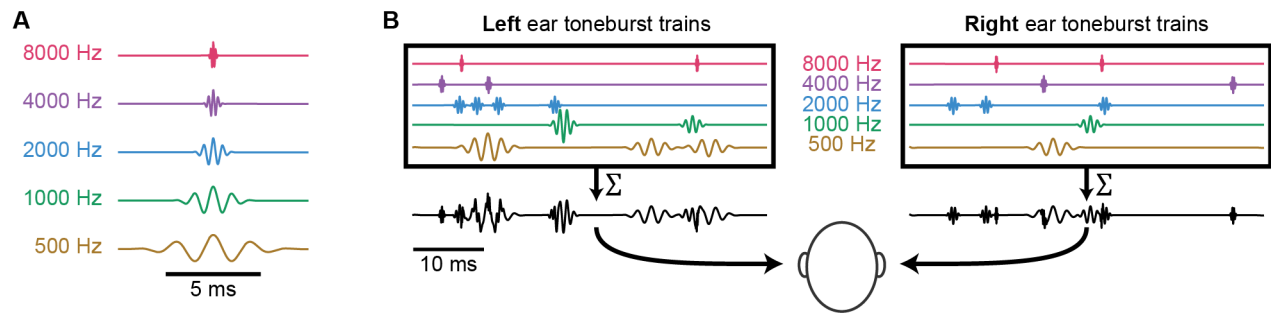145 respectively, from a stimulus epoch.

Figure 1. *pABR stimulus construction. (**A**) Individual toneburst stimuli for each frequency. (**B**) Toneburst trains in each ear (colored lines) are summed to create a two-channel (left, right) stimulus epoch (black lines).*

146

Toneburst stimuli

148 Toneburst stimuli were constructed at frequencies of 500, 1000, 2000, 4000, and 8000 Hz. For each
149 frequency, five cycles of a cosine were multiplied by a Blackman window of the same length, such that the
150 peak of the window was aligned with a maximum of the cosine function (Figure 1A). Consequently,
151 individual tonebursts had durations of 10, 5, 2.5, 1.25, and 0.625 ms for each of the five frequencies,
152 respectively. Stimuli were generated at a sampling rate of 48 kHz to ensure that the highest stimulus
153 frequencies were well below the Nyquist rate. Stimuli were represented in memory as 32-bit integers so
154 that the full dynamic range could be tested without risk of quantization distortion.

155 A 1000 Hz sinusoid test tone was used to calibrate the amplitude of the toneburst stimuli. The tone was
156 played from the tube of the insert earphones (ER-2, Etymotic Research) into the sound level meter (2240,
157 Bruel & Kjaer) using a 2cc acoustic coupler (RA0038, G.R.A.S.) and its digital amplitude was adjusted so
158 that its intensity read 80 dB SPL. The amplitude of this sinusoid served as the reference for matching
159 amplitudes of the toneburst cosine components to give a toneburst stimulus level of 80 dB peak-equivalent
160 SPL (peSPL). Other stimulus levels (L) in dB peSPL were obtained by multiplying the reference-level
161 toneburst by $10^{(L - 80) / 20}$.

162

Toneburst trains with randomized stimulus timing

164 Toneburst trains for each frequency were formed by creating an impulse train with random timing at an
165 overall rate of 40 stimuli / s, and then convolving the impulse train with the toneburst. To construct an
166 impulse train, a vector of zeros was first created with a length of 48,000 samples, corresponding to a 1 s
167 interval. Of these, 40 unique sample indices were chosen at random and the zero replaced randomly with
168 +1 or −1 so that half of the tonebursts in each train were inverted. The impulse train was then convolved
169 with the toneburst, creating a toneburst train with half condensation tonebursts and half rarefaction. Indices
170 of the impulse train too close to the end of the 1 s interval were excluded as possibilities if the toneburst
171 would be truncated. This way each epoch had 40 stimuli but no tonebursts were cut off by the end of the
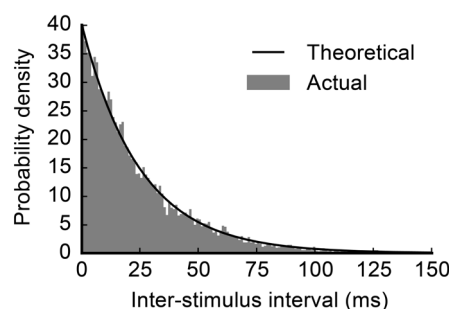172 epoch.

Figure 2. *The distribution of inter-stimulus intervals over all stimuli for λ = 40 stimuli / s (solid gray) compared to the predicted distribution given by $P(t) = 40e^{-40t}$. There is a very close match indicating that the deviations from a true Poisson point process used in this experiment are negligible.*

173 This process of generating each impulse train timing sequences was essentially a one-dimensional
174 homogeneous Poisson point process, with only very subtle differences. Those differences were: 1) the
175 number of stimuli was set exactly to 40, rather than setting the process's rate parameter (typically denoted

5

176 as λ) to 40; 2) the indices were guaranteed to be unique (though they could have been at adjacent
177 samples, or 21 µs apart); 3) because the epochs were 1 s long, the maximum inter-stimulus interval was
178 < 1 s. Figure 2 compares the actual inter-stimulus interval histogram of all toneburst trains with the
179 theoretical exponential distribution of an ideal Poisson process with λ = 40 stimuli / s, demonstrating that
180 they are practically identical.

181

182 *Stimulus epochs*

183 Stimulus epochs lasting 1 s were composed of a combination of 10 toneburst trains (5 frequencies × 2
184 ears). All toneburst trains for the left ear were summed to create the left channel of the stimulus epoch, and
185 the same was done for the right ear (Figure 1B). Each toneburst train was created with a different random
186 seed, such that the timing between any two sequences was completely independent. This statistical
187 independence is what underlies the ability to present stimuli in parallel while acquiring separate responses
188 for each ear-frequency combination.

189 Thirty unique stimulus epochs were generated to ensure sufficient statistical independence between the
190 random processes dictating the toneburst trains (i.e., the impulse trains that were convolved with the
191 tonebursts) for all frequency-ear combinations. Perfect independence between random sequences is
192 achieved with infinite durations. However, modeling undertaken before data were collected determined that
193 30 s sequence durations are enough that any channel interactions are far overpowered by the noise
194 endemic to EEG recording. We used a frozen set sequences for which statistical independence was
195 confirmed.

196

197 *Stimulus artifact mitigation*

198 During construction of the stimulation sequence, we employed a double counter-phasing scheme. First, as
199 described above, the polarity of a random half of the tonebursts in each train were inverted, akin to
200 alternating polarity in periodic stimulation. Second, each of the 30 stimulus epochs were followed in the
201 stimulation sequence by an inverted version of that epoch. Thus, the order of the first six stimulus epochs
202 in the sequence was A^+, A^-, B^+, B^-, C^+, C^-, etc., where A, B, and C denote independent stimulus epochs
203 and the superscript denotes the phase.

204 We also took physical measures to prevent stimulus artifact. We hung earphones from the ceiling so that
205 they were as far from the EEG cap as possible. We also used active cancellation, wherein each earphone
206 attached to another in the same orientation, but with a blocked tube. The dummy earphone received an
207 inverted signal, in order to cancel electromagnetic fields everywhere but close to the transducers. In our
208 experiments this method outperformed passive shielding in artifact reduction, but we note that we have
209 made high-quality recordings without using the dummy earphone method. We also point out that this
210 scheme can be employed in the laboratory, but clinics likely will not (and need not) adopt it.

211

212 *Interleaving trial order*

213 To avoid biases introduced by slow changes in recording quality (e.g., due to changes in subject state or
214 drifting electrode impedances) we interleaved the conditions and consecutively stepped through the trial
215 order. This prevented issues like transient periods of higher EEG noise or slow impedance drifts from
216 singularly affecting one condition over the others.

217

218 Stimulus presentation and EEG recording

219 Scalp potentials were recorded with passive Ag/AgCl electrodes. A positive (non-inverting) electrode was
220 placed just anterior to the vertex at FCz in the standard 10-20 coordinates and plugged into a y-connector
221 which was split into two differential preamplifiers (Brainvision LLC, Greenboro, SC). The two reference
222 (inverting) electrodes were placed on the left and right earlobes (A1 and A2 respectively). The ground
223 electrode was placed at Fpz. Data were recorded at a sampling rate of 10 kHz and high-pass filtered at 0.1
224 Hz during recording, with additional filtering occurring from 30 to 2000 Hz offline using a causal first order
225 Butterworth filter.

6

226 Subjects sat in a comfortable recliner in a darkened sound-treated room (IAC, North Aurora, IL, USA). They
227 were encouraged to relax and to sleep—nearly all subjects slept for at least part of the test, though this
228 was not rigorously measured. All stimuli were presented through insert earphones (ER-2, Etymotic
229 Research, Elk Grove, IL) which were connected to a stimulus presentation system consisting of a sound
230 card (Babyface, RME, Haimhausen, Germany) and a headphone amplifier (HB7, Tucker Davis
231 Technologies, Alachua, FL, USA). A python script controlled stimulus presentation using publicly available
232 software (available at https://github.com/LABSN/expyfun). Digital triggers were sent from the stimulus
233 presentation computer to BrainVision's PyCorder software using the sound card's digital audio out
234 connected to a custom trigger box (modified from a design by the National Acoustic Laboratories, Sydney,
235 NSW, Australia) to precisely mark the start of each stimulus epoch.

236

237 <u>Stimulus conditions used in this study</u>

238 Stimulus level and presentation rate both have important effects on brainstem responses. These factors
239 and their interactions, as well as optimal ranges, are well studied for traditional ABR. However, the effects
240 of simultaneous stimulation across all frequencies with random timing are not obvious. For this proof-of-
241 concept paper we characterized how the responses to pABR stimulation change over an intensity range,
242 and how these responses compare to those from serial presentation at both a high and low intensity.

243 In one session we measured responses in both ears to pABR stimulation with an average presentation rate
244 of 40 stimuli / s and intensities in 10 dB steps between 75 and 25 dB peSPL, for frequencies between 500
245 and 8000 Hz. For a single recording session of 114 minutes, this afforded 16 minutes of recording time per
246 intensity (96 minutes total) to collect 10 responses (5 frequencies each in 2 ears). Three minutes of clicks
247 were also recorded at each intensity but were not analyzed here. Consequently, each averaged response
248 comprised 38,400 repetitions.

249 In a second session we again measured responses to pABR stimulation at a presentation rate of 40
250 stimuli / s. We also recorded responses at interleaved trials to a serial single-frequency condition that used
251 the same toneburst trains but tested each frequency separately. We recorded the pABR and serial ABR to
252 frequencies between 500 and 8000 Hz at both a high and low intensity (75 and 45 dB peSPL). To make
253 this possible in a single session, only the right ear was tested in the serial condition, under the rough but
254 necessary assumption that the left ear would show the same behavior. For a single recording session of
255 108 minutes, this afforded 35 minutes of recording time to collect 20 responses with the pABR (5
256 frequencies in 2 ears at 2 intensities; 15 minutes at 75 dB peSPL and 20 minutes at 45 dB peSPL for a
257 total of 36,000 and 48,000 repetitions respectively), and 69 minutes to collect 10 responses serially (5
258 frequencies in 1 ear at 2 intensities; 26 minutes at 75 dB peSPL and 43 minutes at 45 dB peSPL). More
259 time was allocated for recording serially collected responses to low frequency tonebursts and the lower
260 intensity stimuli, such that recording time per serial condition ranged from 4 minutes (9,600 repetitions) for
261 high intensity and high frequency stimuli (i.e., 2000, 4000, 8000 Hz at 75 dB peSPL) to 15 minutes (36,000
262 repetitions) for 500 Hz at 45 dB peSPL. Four minutes of clicks were also recorded at each intensity but
263 were not analyzed here.

264 Of the 10 total subjects, 2 were able to complete only one of the two sessions, resulting in 9 subjects for
265 each experiment. For the first experiment, one subject's recording was too noisy to see responses and so
266 was excluded, resulting in a final total of 8 subjects for the first session and 9 subjects for the second
267 session.

268

269 <u>Data analysis</u>

270 *Response calculation*

271 During recording, triggers marked the beginning of each 1 s stimulus block, rather than sending a trigger
272 for each toneburst stimulus. This was for two reasons: 1) random stimulation at overall high rates (when all
273 channels are added together) would have resulted in trigger overlaps, and 2) blocks of stimuli can be
274 analyzed in the frequency domain, which makes calculations substantially faster.
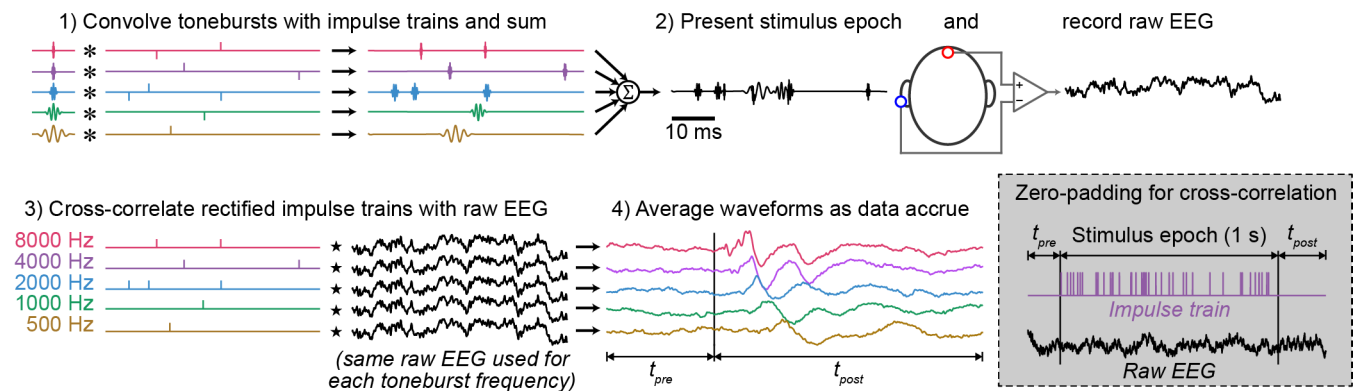
Figure 3. *The analysis chain, shown from stimulus creation and presentation to calculation of response waveforms. For clarity, only a 50 ms time period is shown. Dashed box: Zero-padding scheme shown for a single impulse train of a single epoch. Note t_{pre} and t_{post} are not shown to scale.*

275 Raw EEG data were bandpass filtered between 30 and 2000 Hz (causal, first order Butterworth filter), and
276 then notch-filtered at odd multiples of 60 Hz in that range to remove power line noise. For each stimulus
277 epoch we calculated a single average response to the 40 toneburst stimuli. Rather than calculate the
278 average response directly, however, we used the mathematically equivalent method of cross-correlation,
279 implemented in frequency domain, between the stimulus sequence and the EEG data. Figure 3
280 demonstrates this process. Due to the random nature of the stimuli, we were able to extend the analysis
281 window for each toneburst to be 1 s long, which is much longer than the tens of milliseconds duration for
282 the standard ABR (limited to the reciprocal of the presentation rate). This extended window allowed us to
283 calculate response waveforms for the time period 500 ms before and after each stimulus (i.e., from −500 to
284 500 s, where $t = 0$ is the time of stimulus/toneburst onset). To do this, for each 1 s stimulus block we took
285 the corresponding period of EEG data (1 s) along with the data 500 ms before and after it, leading to 2
286 seconds of EEG data, denoted as y. Then, for each toneburst train, we created a timing sequence by
287 placing a single-sample unit-height impulse corresponding to the start of each toneburst (i.e., from the
288 rectified impulse train created during stimulus construction), and zero-padded it with 500 ms before and
289 after, leading to a 2-second impulse train with all of its impulses located in the middle 1 s, denoted as $x_{f,e}$,
290 where f is the toneburst frequency and e is the ear stimulated. The response waveform, $w_{f,e}$, was
291 computed as the circular cross-correlation of $x_{f,e}$ and y, done in the frequency domain for efficiency, as

292
$$w_{f,e} = \frac{1}{n_s} \mathcal{F}^{-1}\{\mathcal{F}\{x_{f,e}\}^* \, \mathcal{F}\{y\}\},$$

293 where $\mathcal{F}$ denotes the fast Fourier transform, $\mathcal{F}^{-1}$ its inverse, $*$ denotes complex conjugation, and n_s the
294 number of impulses in the sequence. The result is a response where the time interval [0, 500] ms is found
295 at the beginning of $w_{f,e}$ and the interval [−500, 0) ms is found at the end, such that concatenating the two
296 (end first) yields the response over the interval [−500, 500] ms (the middle 1 s of $w_{f,e}$ is discarded). This
297 process was repeated for each of the ten toneburst trains (5 frequencies, 2 ears) for each epoch. This
298 equation assumes y is a single EEG channel, a common scenario for ABR, but this analysis can simply be
299 repeated for each channel if more than one is present. In this study we recorded from two channels, but
300 then averaged the calculated responses for further analysis because we were not concerned with
301 ipsilateral versus contralateral differences for the purposes of this paper. However, separately analyzing
302 ipsilateral and contralateral responses for clinical applications would be easy to perform by keeping the two
303 channels separate rather than averaging. It should also be noted that the typical per-stimulus epoching and
304 averaging in the time domain could have been employed and yields identical results but at greater
305 computational cost.

306

307 *Response averaging*

308 Because the quality of the ABR waveforms as a function of acquisition time was of interest, we calculated
309 the cumulative averaged response after each 1 s stimulus block. To account for variations in noise levels
310 over time (either slow drifts or due to transient sources like movement artifacts), we weighed each
311 response according to the inverse of the noise in that epoch. This process is the same in principle as

312 Bayesian averaging described by Elberling and Wahlgreen (1985), but the noise variance was calculated
313 differently. We computed the variance of the pre-stimulus window in the time period −480 ms to −20 ms.
314 We then weighed each epoch by the inverse of its variance relative to the sum of the inverse of variances
315 of all epochs

316
$$g_i = \frac{1/\sigma_i^2}{\sum_{i=1}^n 1/\sigma_i^2},$$

317 where i is the epoch number and n is the number of collected epochs. The averaged response was then
318 calculated as

319
$$w = \sum_{i=1}^n g_i w_i.$$

320 This averaging process avoids the need for artifact rejection based on thresholds, and also takes
321 advantage of the long pre-stimulus window afforded by randomized timing sequences to give a better
322 estimate of the noise.

323

324 *SNR calculation*

325 The SNR of a waveform was estimated by comparing the variance (i.e., mean-subtracted energy) of the
326 waveform in the 10 ms latency range starting at a lag that captured wave V for that frequency (500 Hz:
327 10.5 ms, 1000 Hz: 7.5 ms, 2000 Hz: 6.5 ms, 4000 and 8000 Hz: 5 ms; Stapells, 2011). That period
328 contained signal and noise, so its variance is denoted σ_{S+N}^2. We estimated the noise variance, σ_N^2, by
329 segmenting the pre-stimulus baseline between −480 and −20 ms into 10 ms intervals, finding the variance
330 of each one, and computing the mean. We then computed the SNR in decibels for every waveform as

331
$$SNR = 10\log_{10}\left[\frac{\sigma_{S+N}^2 - \sigma_N^2}{\sigma_N^2}\right].$$

332

333 **RESULTS**

334 <u>The pABR yields canonical waveforms that characteristically change over a range of intensities</u>

335 We recorded the pABR over a range of stimulus levels from 75 to 25 dB peSPL in 10 dB steps. Figure 4
336 shows the grand average and responses from two example subjects. Overall response morphology
337 strongly resembled those yielded by traditional methods.

338 Aspects of response morphology were quantified by a trained audiologist (MJP) who manually inspected
339 each waveform to determine the presence, amplitude and latency of wave V. The same measures were
340 quantified by the other author (RKM) in 38% of responses. The intraclass correlation coefficient (ICC3) for
341 each frequency and measure was ≥ 0.9 (all p < 0.001), indicating excellent reliability for chosen wave V
342 peak latencies and amplitudes. We modeled wave V latency (Figure 5A) and amplitude (Figure 5B) using
343 two linear mixed effects models, each with a random intercept for each subject and fixed factors of ear,
344 stimulus level, stimulus frequency in log units, and the interaction for log frequency and stimulus level.
345 Wave V latency showed no difference between ears (p = 0.66) but there were significant effects of level,
346 frequency, and a significant level-frequency interaction (all p < .001), indicating that latency decreased with
347 increasing level and increasing frequency, and the effect of intensity was greater at lower frequencies.
348 Wave V amplitude increased with stimulus level (p < .001) and this increase was greater for higher
349 frequencies (significant level-frequency interaction, p < .001). These trends are clearly visible in Figure 5,
350 and are generally consistent with traditional ABR (Burkard, Don, & Eggermont, 2006).

351

352 While we did not quantify the presence of waves other than wave V, Figure 4 also shows that both waves I
353 and III are clearly visible at higher frequencies in the grand average as well as typical individual responses.
354 Measuring wave I rapidly and at the moderate intensities used in this study may have applications to the
355 study of hidden hearing loss (Liberman, Epstein, Cleveland, Wang, & Maison, 2016).
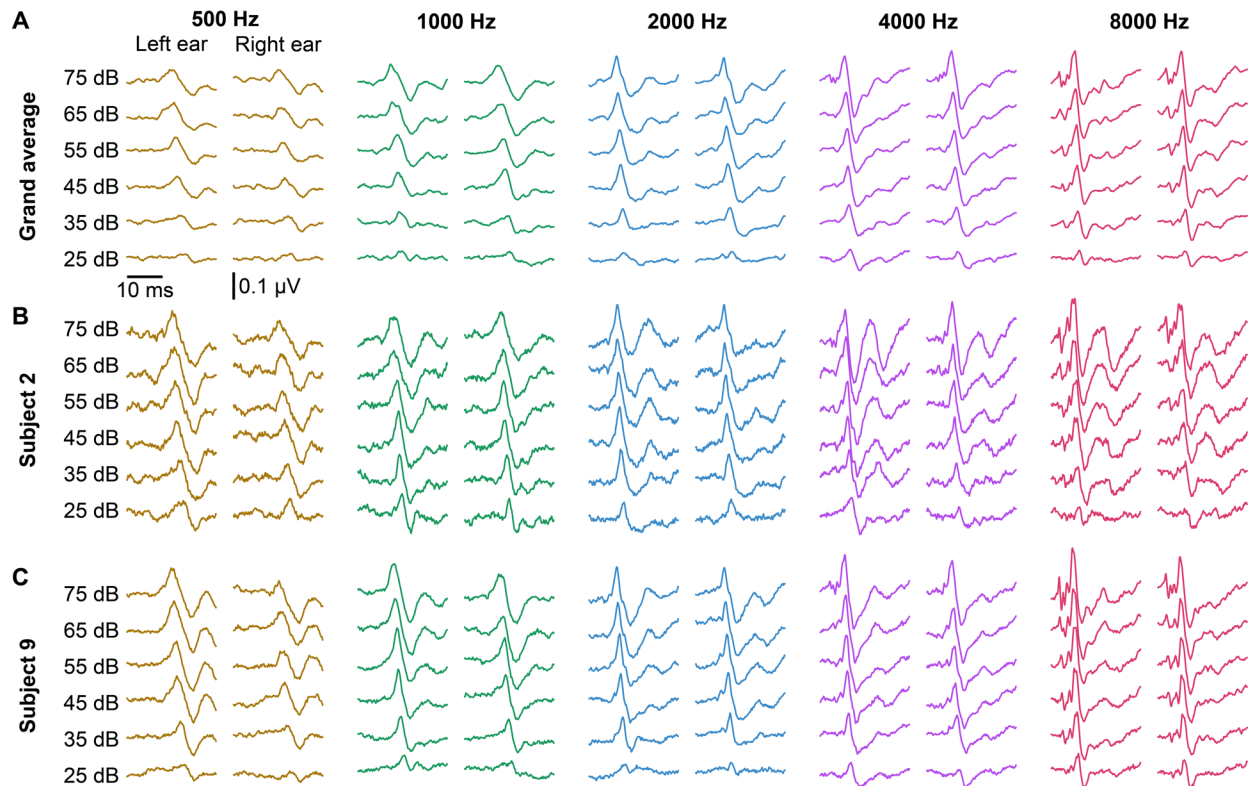
9

Figure 4. *Intensity series waveforms across frequencies and for the left and right ears. (**A**) Grand average of 8 subjects. (**B**,**C**) Two example subjects' responses. All responses are plotted over the interval 0 to 25 ms.*

356   We thus found that the pABR gives typical ABR waveforms over a range of frequencies and intensities and
357   recapitulates the effects of stimulus frequency and intensity on response morphology seen in traditional
358   ABR. In the next section we directly compare pABR with serially recorded responses recorded in the same
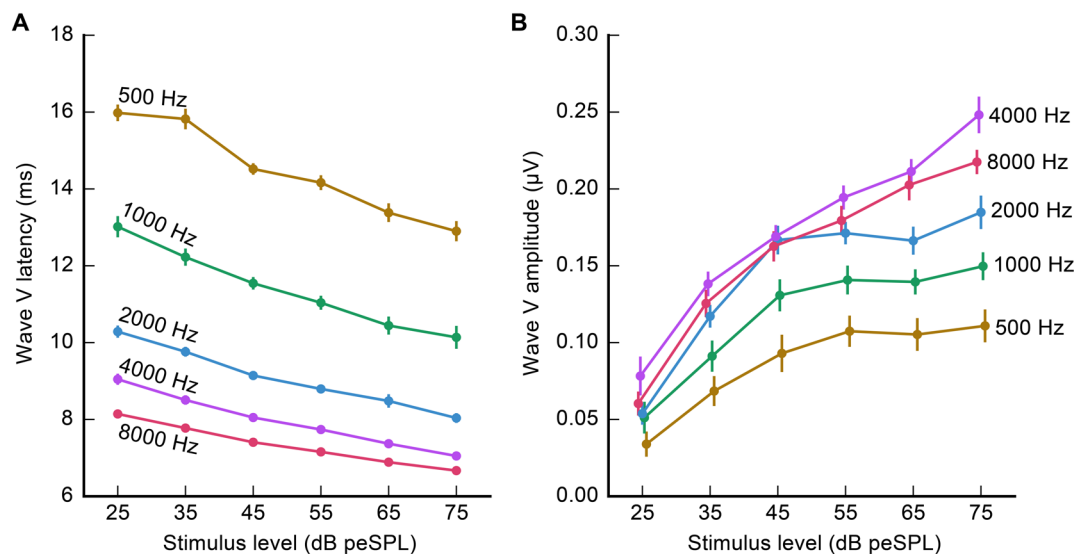359   subject in a single session.

Figure 5. *Mean wave V latency (**A**) and amplitude (**B**) as a function of intensity. Stimulus frequency is indicated on each line. Error bars (where large enough to be seen) indicate ±1 SEM. Lines have a slight horizontal offset in **B** to reduce overlap.*

360

361 <u>pABR and serial response waveforms differ in latency and amplitude at high intensities</u>

362 We recorded responses in 9 subjects (8 of whom also participated in the previous experiment) to stimulus
363 trains presented in parallel (all frequencies, both ears), versus the same stimulus trains presented serially
364 (one frequency, one ear). Due to time constraints, serial responses could only be recorded in one ear
365 (right), and so even though the pABR recorded responses in both ears, only the right ear responses were
366 compared. Responses were measured for a high and low intensity (75 and 45 dB peSPL respectively).
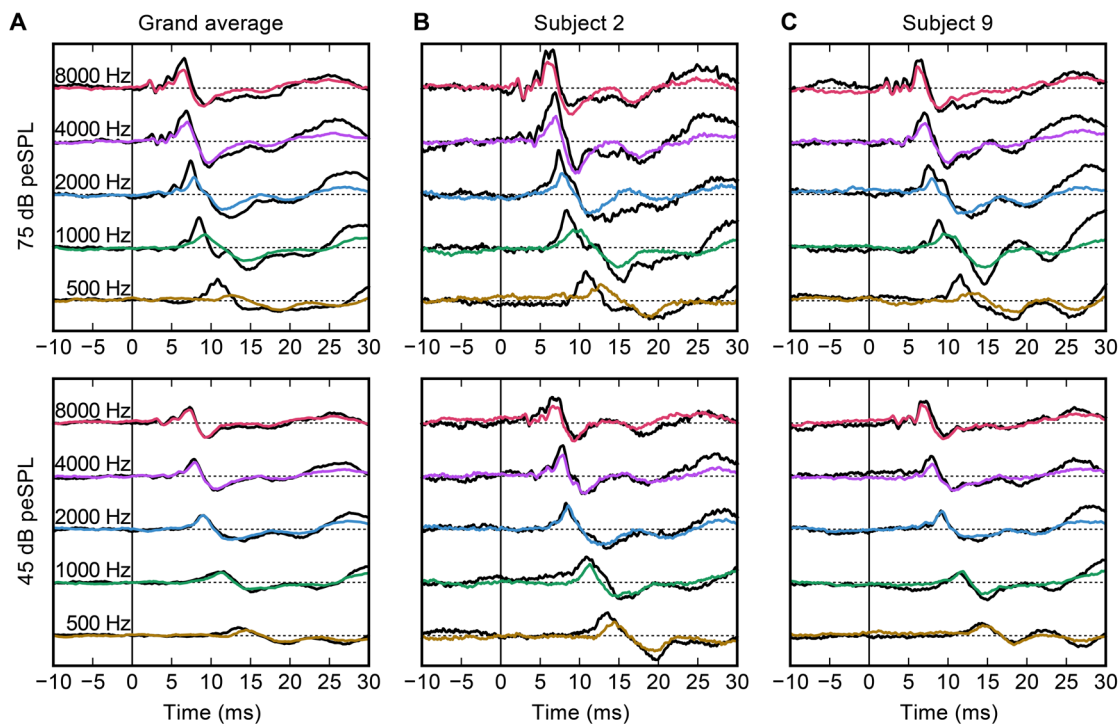

Figure 6. *Parallel vs series acquisition waveforms (right ear only).* **(A)** *Grand average.* **(B,C)** *Example subjects. pABR is shown in colored lines. Corresponding serial waveforms are shown in black. Vertical spacing is 0.3 μV / div.*

367 Figure 6 shows grand averaged responses and responses from two subjects for pABR (colored as in other
368 figures) and the corresponding serial responses (black). Each overlapping waveform is a response to the
369 same stimuli that only differ in the presentation context (parallel, with other stimuli simultaneously present,
370 versus serial, with stimulus trains presented in isolation). Overall waveform morphology of responses were
371 similar using both methods, with some differences in wave V amplitude and latency, described in detail
372 below.

373 Wave V peak latency and amplitude were further quantified and are displayed for pABR versus serial ABR
374 acquisition in Figure 7. Again, we showed good agreement in our wave V choices (all ICC3 ≥ 0.89, $p <$
375 0.001). Linear mixed effects models of wave V latency and amplitude were used again with a random
376 intercept for subject and fixed factors of method (pABR versus serial), stimulus level (75 and 45 dB
377 peSPL), log frequency, as well as the full set of two and three-factor interactions. Latency (Figure 7A)
378 showed significant effects of stimulus level ($p = .012$) and frequency ($p < .001$) as well as the method-level-
379 frequency interaction ($p = .004$). Thus, as expected, latencies were longer at lower frequencies and levels.
380 In addition, latencies were longer for pABR than serial ABR for lower frequencies at higher levels. This
381 interaction trend is also clearly visible in the 500 Hz 75 dB peSPL waveforms of Figure 6 for the grand
382 averages and both example subjects. For amplitude (Figure 7B), only the two-way interaction of method
383 and level was significant ($p = 0.032$), indicating that serial ABR shows larger wave V amplitudes at the
384 higher stimulus level. The significant interaction terms of the latency and amplitude models are both
385 consistent with potentially improved place specificity afforded by pABR, a notion which receives a fuller
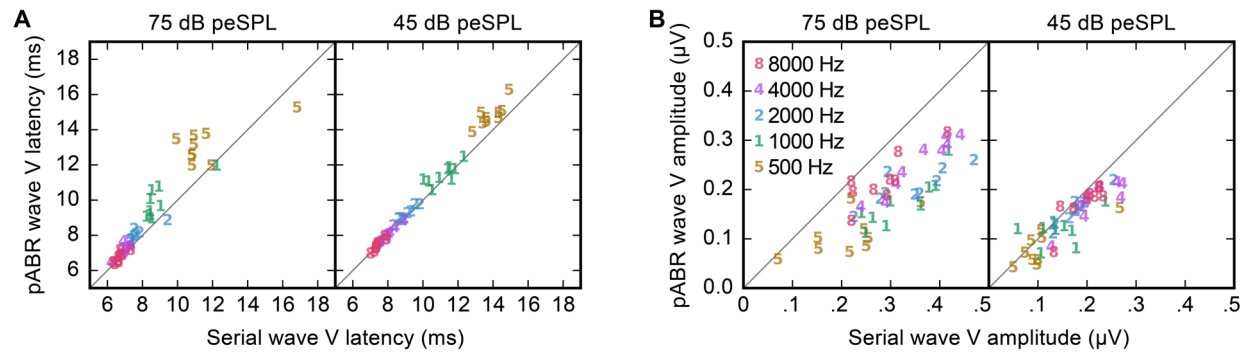386 explanation in the Discussion section.

Figure 7. *Comparison of pABR with serial wave V latency (**A**) and amplitude (**B**) for all subjects (N = 9) at each frequency for both stimulus levels. Quantities shown are for the right ear. Stimulus frequency indicated by marker number and color.*

387

Acquisition times are faster for pABR than serial measurement

389 Having compared waveform morphology and demonstrated that pABR provides canonical waveforms with
390 only minor systematic differences in wave V amplitude and latency, we next compared the acquisition time
391 of pABR to serial measurements.

392 First we characterized the time (in minutes) it took to reach a residual noise of 20 nV, which was calculated
393 for each waveform as the square root of σ_N^2. For pABR recording, the time for the responses across all
394 frequencies to reach criterion was defined as the time taken by the slowest response to reach 20 nV (i.e.,
395 the maximum time across all responses). For serial measurement, the acquisition time was the sum of the
396 times for each of the five frequencies' responses to reach criterion, doubled to account for the other ear.
397 We calculated the time to the 20 nV residual noise criterion for all subjects at both stimulus levels, leading
398 to 18 estimates for each acquisition method, which are plotted as a histogram in Figure 8. The pABR
399 reached 20 nV for all waveforms with a median time of 4.6 minutes (3.8–5.4 minutes interquartile range).
400 Serial recordings, on the other hand, took substantially longer at 30.1 minutes (23.8–40.0 minutes).
401 Dividing each serial time by each corresponding pABR time yielded a median speedup ratio of 6.0 (5.7–6.6
402 interquartile range), indicating a large advantage for the pABR.
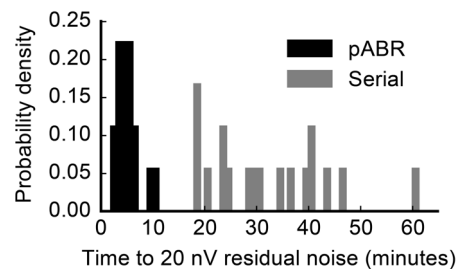

Figure 8. *Comparison of time to reach 20 nV residual noise for all 10 waveforms between methods (pABR in black, serial in gray). Two intensities for 9 subjects are shown, leading to 18 data points for each acquisition method.*

403 The residual noise numbers indicate that in situations where multiple waveforms are desired, recording
404 them in parallel leads to lower noise levels much faster than recording them one at a time. If pABR yielded
405 identical responses to serial measurement, then the speedup ratios for response acquisition would be
406 higher. However, because the pABR leads to smaller responses in some situations (low frequencies at
407 high intensities), the speedups were less pronounced, particularly at higher intensities.

408 Second, we further compared estimated acquisition times by calculating the time required for all waveforms
409 of a given intensity to reach 0 dB SNR[1]. As with the residual noise estimates, the total acquisition time for
410 pABR was the time it took for the last waveform to reach threshold, and the total time for serial acquisition
411 was the sum of acquisition times for all waveforms (here approximated as the total for one ear, doubled).

---

[1]The choice of 0 dB as the SNR threshold was arbitrary and based on visual assessment of when waveforms looked "good." Changing this threshold would have changed the acquisition times. This change, however, would be multiplicative, such that the speedup ratios—our measure of how much faster the pABR is—would be unaffected.

412 These times are given for all subjects in Table 1, and Figure 9A shows an example acquisition run modeled
413 from one subject's data for demonstration purposes. At 75 dB peSPL, the median acquisition time for
414 pABR was 1.93 minutes (0.93–3.63 minutes interquartile range) and for serial acquisition was 1.45 minutes
415 (0.94–3.45 minutes interquartile range). Parallel acquisition was faster for 5 of 9 subjects, with a median
416 pABR speedup ratio of 1.45 (0.89–1.64). At 45 dB peSPL the acquisition time difference was pronounced:
417 median acquisition time for pABR was 4.60 minutes (1.86–8.99 minutes) versus 7.81 minutes (5.95–9.92
418 minutes) for serial presentation. At this lower intensity, pABR was faster than serial recording for all 9
419 subjects, with a median pABR speedup ratio of 2.99 (1.12–3.92 interquartile range). A scatterplot
420 comparing the pABR and serial acquisition times at 75 and 45 dB peSPL (filled and open circles,
421 respectively) is shown in Figure 9B. Points below the unity line indicate a pABR advantage.

422

			S2	S3	S5	S6	S7	S8	S9	S10	S11	LQ	MED	UQ
75 dB peSPL	Parallel	500 Hz	0.41	4.91	1.93	3.00	22.56	0.99	0.93	0.50	3.63	0.93	1.93	3.63
		1000 Hz	0.35	0.68	0.97	0.60	2.39	0.36	0.24	0.21	1.40	0.35	0.60	0.97
		2000 Hz	0.36	0.54	0.70	0.91	1.89	0.19	0.29	0.40	0.51	0.36	0.51	0.70
		4000 Hz	0.17	0.64	0.26	0.32	1.82	0.16	0.27	0.30	0.31	0.26	0.30	0.32
		8000 Hz	0.20	0.66	0.44	0.64	2.88	0.27	0.28	0.25	0.66	0.27	0.44	0.66
		Total (MAX)	0.41	4.91	1.93	3.00	22.56	0.99	0.93	0.50	3.63	**0.93**	**1.93**	**3.63**
	Serial	500 Hz	0.18	0.73	0.61	0.27	14.24	0.35	0.15	0.09	0.79	0.18	0.35	0.73
		1000 Hz	0.06	0.19	0.27	0.06	0.77	0.12	0.05	0.07	0.22	0.06	0.12	0.22
		2000 Hz	0.07	0.19	0.16	0.13	0.79	0.08	0.07	0.05	0.14	0.07	0.13	0.16
		4000 Hz	0.05	0.32	0.15	0.10	0.74	0.08	0.06	0.08	0.21	0.08	0.10	0.21
		8000 Hz	0.11	0.41	0.43	0.16	0.66	0.09	0.08	0.11	0.36	0.11	0.16	0.41
		Total (2×SUM)	0.94	3.68	3.23	1.45	34.40	1.44	0.82	0.82	3.45	**0.94**	**1.45**	**3.45**
45 dB peSPL	Parallel	500 Hz	0.57	8.99	1.44	7.76	8.78	1.86	0.83	4.60	53.12	1.44	4.60	8.78
		1000 Hz	0.47	1.76	3.04	1.31	7.79	0.86	0.58	0.82	1.73	0.82	1.31	1.76
		2000 Hz	0.23	0.62	1.10	1.03	3.69	0.31	0.29	0.50	1.01	0.31	0.62	1.03
		4000 Hz	0.41	0.93	0.47	0.71	9.26	0.25	0.32	0.50	0.69	0.41	0.50	0.71
		8000 Hz	0.57	1.54	0.65	0.84	10.34	0.30	0.30	0.45	1.10	0.45	0.65	1.10
		Total (MAX)	0.57	8.99	3.04	7.76	10.34	1.86	0.83	4.60	53.12	**1.86**	**4.60**	**8.99**
	Serial	500 Hz	0.15	1.71	1.99	1.56	11.64	2.11	0.84	0.89	20.17	0.89	1.71	2.11
		1000 Hz	0.13	0.60	0.37	0.83	6.00	0.98	0.48	0.91	7.12	0.48	0.83	0.98
		2000 Hz	0.15	0.51	1.00	0.67	5.52	0.18	0.32	0.42	0.77	0.32	0.51	0.77
		4000 Hz	0.22	0.85	0.53	0.37	4.50	0.16	0.21	0.45	0.53	0.22	0.45	0.53
		8000 Hz	0.21	1.29	0.66	0.47	2.81	0.20	0.23	0.31	1.21	0.23	0.47	1.21
		Total (2×SUM)	1.72	9.92	9.10	7.81	60.94	7.27	4.16	5.95	59.60	**5.95**	**7.81**	**9.92**

	S2	S3	S0	S6	S7	S8	S9	S10	S11	LQ	MED	UQ
Speedup 75 dB peSPL	*2.30*	*0.75*	*1.68*	*0.48*	*1.52*	*1.45*	*0.89*	*1.64*	*0.95*	*0.89*	*1.45*	*1.64*
Speedup 45 dB peSPL	*3.00*	*1.10*	*2.99*	*1.01*	*5.90*	*3.92*	*5.03*	*1.29*	*1.12*	*1.12*	*2.99*	*3.92*

423

424 **Table 1.** *Time to 0 dB SNR (in minutes) for each subject as well as the median and quantiles. For each method at each stimulus*
425 *level the time is shown for all frequencies, with the total (computed with the appropriate method) shown below. Shown at the*
426 *bottom in italics are the speedups for both stimulus levels. These numbers are unitless ratios, rather than minutes, where higher*
427 *numbers represent an advantage for the pABR over the serial ABR.*

428 Even in the case where a pABR and corresponding serial acquisition take the same amount of time, there
429 is a secondary SNR advantage for pABR which comes from the criterion that ends each run. For the pABR,
430 data continues to accrue for all waveforms while waiting for the last response to reach criterion. Therefore,
431 at the end of the run all but the slowest waveform will have an SNR better than the stopping criterion. In
432 contrast, for serial acquisition, at the end of the run all waveforms will have just reached criterion SNR. This
433 difference can be seen in Figure 9A, where at the end of the parallel run (double black line at time 1:55) all
434 but the 500 Hz right ear response are better than 0 dB SNR. This pABR SNR benefit can be quantified by
435 examining the SNR of the pABR waveforms at the time point when the corresponding serial run completed
436 (red dashed line at time 8:34). These SNR benefits are plotted in Figure 9C for all frequencies at both
437 intensities. At 75 dB peSPL, the median SNR benefits for 500 through 8000 Hz are 1.6, 5.4, 6.6, 7.6, 7.2
438 dB. For lower intensity of 45 dB peSPL, the benefits are even greater: 4.8, 8.6, 11.6, 10.7, 11.2 dB from
439 500 to 8000 Hz. These improvements potentially allow much better assessment of waveform morphology,
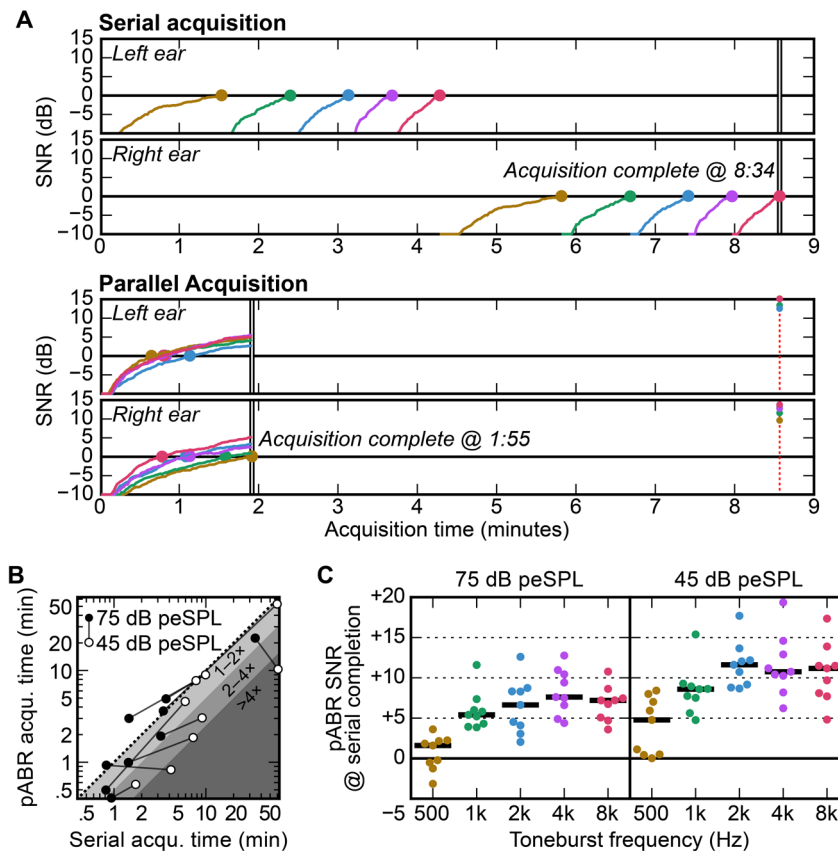440 such as the presence and size of wave I.

Figure 9. pABR shows faster acquisition and better SNR. (A) Real-time acquisition runs simulated from offline data for one subject at 45 dB peSPL. For serial ABR, unrecorded left ear runs were assumed to be equal to right ear. (B) Comparison recording time for 9 subjects. Points below dotted unity line are cases where pABR is faster. Shaded regions indicate speedup ratios of 1–2 (light gray), 2–4 (medium gray), and > 4 (dark gray). (C) SNR of pABR runs upon serial acquisition completion (subjects colored points, median black lines), corresponding for one subject to the points on the red dashed vertical line in A.

441

DISCUSSION

443 Here we describe the pABR, a new method for recording the frequency-specific ABR to multiple
444 simultaneous stimulus trains at several octave frequencies in both ears. The pABR yields waveforms with
445 canonical response components, namely wave V, albeit at slightly different latencies and amplitudes at
446 higher intensities. The principal advantage of the pABR is that low noise levels are achieved in drastically
447 shorter times, which leads to faster acquisition times. Faster response acquisition will yield shorter clinic
448 visits, or visits of the same length that yield much better estimates of the hearing thresholds on which
449 crucial clinical decisions are based. Furthermore, octave frequencies from 500 to 8000 Hz can be obtained
450 in comparable or shorter lengths of time, which provides a more comprehensive assessment of hearing
451 function than typically achieved in current clinical practice. At best, 500–4000 Hz thresholds are currently

452 achieved but more often only 500, 2000 and maybe 4000 Hz are obtained (American Academy of
453 Audiology, 2012; BC Early Hearing Program, 2012; Hyde, 2008). The most obvious question about the
454 pABR—how *much* faster it is—is also the most difficult to answer because it depends on a multitude of
455 factors. We discuss several of these factors below.

456 The estimate of acquisition time we used here—time to criterion SNR—was objective but most useful for
457 relative comparisons between the methods rather than absolute estimates of acquisition time. First, the
458 choice of SNR has a large effect on the time in minutes (using +3 dB instead of 0 dB would have doubled
459 all the times, for instance), so the times reported here should be considered within the context of our
460 chosen criterion. However, a change in criterion would not affect the speedup ratios. These ratios indicate
461 that the pABR can yield 10 good waveforms about 3 times faster than the serial ABR in at least half the
462 cases (Table 1). This means more information could be collected in an appointment, or the same amount
463 of information could be collected quicker. For some subjects, acquisition of 10 waveforms occurred quickly,
464 with times as low as less than half a minute (Table 1). For the pABR at a level closer to threshold (i.e., 45
465 dB peSPL), 5 of 9 subjects achieved good waveforms within 5 minutes, compared to only 2 subjects with
466 serial presentation. As would happen in the clinic, there were some subjects that had noisier responses
467 and took substantially longer to acquire 10 waveforms with both parallel and serial presentation, such as
468 two subjects who achieved waveforms in estimated times of about 53 (pABR) and 61 (serial) minutes. The
469 pABR is subject to the effects of noisy testing situations, just as the serial ABR. However, these time
470 estimates may also be conservative given the automatic calculation of SNR. Importantly, audiologists are
471 highly trained at recognizing response components. For example, in many cases while analyzing our data
472 we could see a clear 500 Hz response when the SNR was still below our 0 dB SNR criterion. For those
473 subjects who had estimated times to 0 dB SNR greater than 10 minutes, a trained audiologist would likely
474 detect the presence or absence of a waveform earlier and make decisions about moving on to another
475 level. Testing with trained clinicians interpreting waveforms as they are acquired in real time will give more
476 meaningful time estimates in minutes.

477 The pABR offers advantages that will make clinicians' decisions about response presence more accurate
478 and easier to make. First, viewing the response to a specific frequency in context of the other frequencies
479 being simultaneously acquired allows the clinician to make a better, holistic assessment of its
480 presence/absence than viewing the same waveform in isolation. Second, extending the analysis window
481 (made possible by the random stimulus timing) can show later response components, such as the middle
482 latency response (MLR), which when present can further eliminate uncertainty whether a response is
483 present or absent. Our focus was on the ABR, but extending the signal beyond 10 ms to include the MLR
484 will improve SNR estimates and may also further decrease acquisition times based on time to 0 dB SNR.
485 Including the MLR may have shortened the long acquisition times estimated for the particularly noisy
486 subjects discussed above (see Table 1). The pre-stimulus period can also be extended, giving a better
487 impression of the noise. These advantages are highlighted in Figure 10. In panel A, the 500 Hz response is
488 shown on its own. A response may be present, but its amplitude is only slightly greater than that of the
489 noise. In panel B, the same response is shown along with the other simultaneously recorded frequencies
490 for that ear, making the 500 Hz response easier to see. In panel C, the extended analysis window provides
491 a clearer pre-stimulus baseline and middle latency components at ~35 ms that make the presence of a 500
492 Hz response more certain. The use of latencies beyond the typical ABR window will be an important
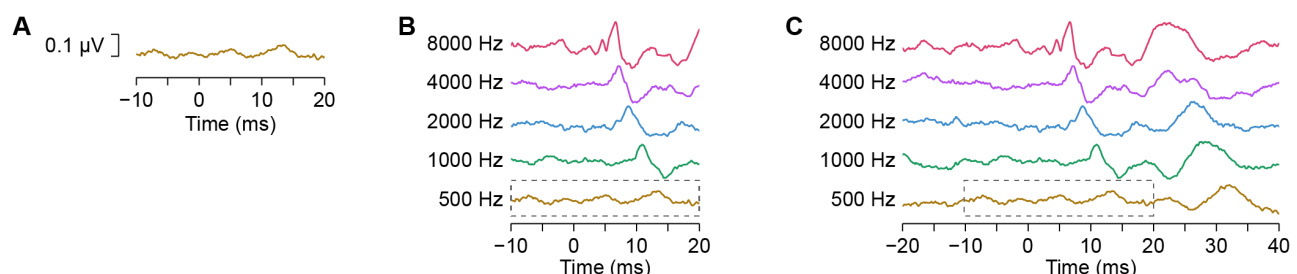493 subject of future investigation.

Figure 10. Improved visual response detection. (A) 500 Hz response waveform alone. (B) Same response with other frequencies simultaneously acquired. Dotted gray box surrounds the waveform from A. (C) 500 Hz response with other frequencies present and analysis window extended 10 ms to the left and 20 ms to the right. Gray box as in B.

494 The hearing thresholds of the people being tested will also have a large effect on the overall measurement
495 time. In the present study all subjects had normal hearing thresholds, and 500 Hz was the most difficult

496 response to acquire. This is not surprising, and even during current diagnostic exams normal hearing for
497 500 Hz is determined using a higher level than the other frequencies (American Academy of Audiology,
498 2012; BC Early Hearing Program, 2012; Hyde, 2008). However, high frequency sloping loss is the most
499 common configuration (e.g., Pittman & Stelmachowicz, 2003). Thus, while the pABR's speed advantage
500 was limited by the low frequency acquisition time here, this may not be true in most cases where a hearing
501 loss is present. At higher levels necessary to determine high frequency thresholds, the level for 500 Hz
502 would be suprathreshold and generate responses with larger SNRs quicker than at a level near threshold
503 (e.g., time to 0 dB SNR for 75 versus 45 dB peSPL in Table 1, Figure 9B). Consequently, the actual
504 acquisition time could be further reduced relative to traditional methods. Additionally, because the pABR
505 reaches low residual noise levels faster than traditional methods, the pABR may allow clinicians to more
506 quickly determine "no response" when none is present.

507 There are thus several factors that limit our ability to fully predict the absolute speed gains the pABR will
508 provide in the clinic. Even non-measurement times between runs will be reduced because the clinician
509 need only select the next intensity to test, rather than choosing a specific intensity-frequency-ear
510 combination as the next step of the threshold search. We show here that the pABR is faster than traditional
511 methods and offers a number of factors that may further improve the speedup. The next step to quantifying
512 the full advantages for clinical use will involve testing the pABR in an actual clinical setting with the patients
513 of interest—namely people (adults, infants, and children) with a wide range of hearing loss.

514 The pABR is not the only objective audiometric tool that allows simultaneous threshold estimation at
515 multiple frequencies—this is also accomplished by the multiple ASSR. As such, the ASSR warrants
516 comparison with the pABR. The ASSR is an evoked response that is phase-locked to a periodic stimulus
517 and can also be measured with most ABR hardware. In clinical settings, the stimulus is typically a tonal
518 carrier at the test frequency (e.g. 500 Hz) whose amplitude is modulated to create the steady-state
519 response. Modulation frequencies in the 80–100 Hz range are used to avoid contributions from cortical
520 generators which are affected by subject state (Korczak, Smart, Delgado, Strobel, & Bradford, 2012). As
521 with the toneburst ABR, correlations between ASSR and behavioral thresholds reach around 0.9 when a
522 large range is considered (Luts et al., 2006). More than one frequency and ear can be tested at a time by
523 "tagging" them with different modulator frequencies. Rather than waveforms, however, the ASSR
524 assessment is based on a scalar measure of its phase-locking to the modulator (and its harmonics),
525 expressed as a single summary quantity. In contrast, the pABR provides full response waveforms. This
526 carries a number of advantages: 1) it allows inference beyond the presence or absence of a response,
527 such as the investigation of auditory neuropathy and site-of-lesion testing, 2) it allows the separation of
528 brainstem and cortical responses by their latencies, letting the clinician use middle latency cortical
529 responses if present, and 3) it will require less training because it draws on clinicians' existing expertise in
530 interpreting ABR waveforms.

531 Because the pABR tests multiple frequencies at once, the potential for interactions between stimuli in the
532 cochlea must be considered. Even though highly frequency-specific stimuli can be generated, they may not
533 elicit place-specific displacements along the basilar membrane when presented without masking (as is
534 typical). High intensity stimuli elicit broader excitation patterns (Robles & Ruggero, 2001) and excitation
535 asymmetrically spreads towards the base of the cochlea. Therefore, responses to low-frequency stimuli
536 include greater contributions from other parts of the cochlea with higher best frequencies. However, the
537 pABR has the potential to provide better place-specific responses because each of the frequency bands
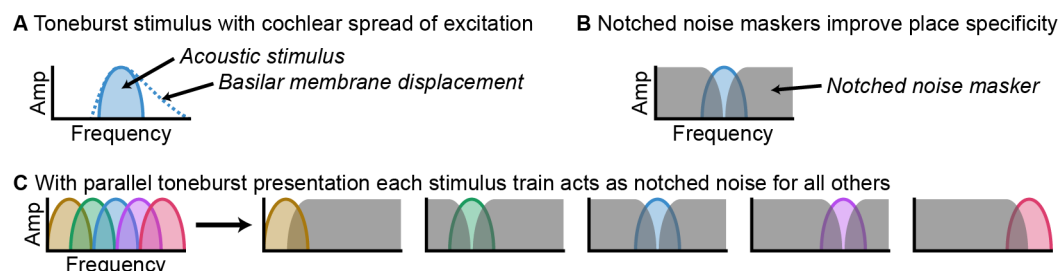
Figure 11. *Parallel stimulation allows toneburst trains to also function as notched noise. (**A**) Cartoon representation of a single toneburst stimulus in the frequency domain (filled area), and the pattern of excitation it evokes in the cochlea (dashed line), showing spread of excitation towards the basal end. (**B**) Notched noise can be used to mask the off-frequency excitation, yielding a more place-specific response. (**C**) In pABR, each frequency band is masked by the others, which summed have a similar effect to a notched noise masker.*

16

538 could act as masking noise for all the others, as depicted in Figure 8. Essentially, the pABR could act akin
539 to recording a series of masked ABRs but in one run. Evidence that may support this place-specific
540 hypothesis comes from the prolonged latencies for the pABR relative the serially recorded responses,
541 especially for the lower frequencies at higher intensities (Figures 6 and 7). Because spread of excitation is
542 greater at higher intensities, we would expect to see the biggest differences between pABR and serial ABR
543 at higher levels. Indeed, we found that at the lower level of 45 dB peSPL, there was no difference between
544 the two methods in wave V amplitude or latency, indicating minimal interference. However, at the higher
545 stimulus level of 75 dB peSPL, wave V amplitude was reduced and wave V latency longer for pABR than
546 serial ABR for the lower frequencies. These differences for lower frequencies are consistent with basal
547 spread of activation contributing to responses in the traditional ABR but being masked under the pABR.
548 Thus, at lower stimulus levels, where acquisition generally takes longer and speedups are the most
549 needed, interactions between bands of the cochlea do not seem to be an issue. At higher levels
550 interactions appear to be present, likely leading to more modest speedups, but potentially in exchange for
551 (or because of) improved place specificity.

552 In summary, the pABR is a viable method for recording canonical ABR waveforms at a fraction of the time
553 of traditional serial methods, particularly for lower intensity stimuli. Consequently, the pABR has great
554 potential for facilitating quick and accurate hearing threshold estimation that is important for timely
555 diagnosis and treatment of hearing loss. Furthermore, the advantages of extended analysis windows
556 afforded by randomized timing allows better noise estimates and inclusion of additional peaks such as the
557 MLR, which will improve SNR estimates. Finally, our results suggest that the masking provided by
558 simultaneously presented tonebursts might mitigate spread of activation at higher intensities, with potential
559 improvements in place specificity. Future studies will focus on investigating optimal parameters for the
560 pABR to estimate thresholds, modeling place specificity of the pABR, and assessing the utility of the pABR
561 for estimating thresholds for various configurations of hearing loss with patients in the clinic.

562

571

572 **DATA AVAILABILITY**

573 Data will be made available upon reasonable request to the corresponding author.

REFERENCES

574

575 American Academy of Audiology. (2012, August). *Assessment of Hearing in Infants and Young Children*.

576 BC Early Hearing Program. (2012). *Audiology Assessment Protocol*. Retrieved from
577   http://www.phsa.ca/Documents/bcehpaudiologyassessmentprotocol.pdf

578 Brambrink, A. M., Evers, A. S., Avidan, M. S., Farber, N. B., Smith, D. J., Martin, L. D., … Olney, J. W.
579   (2012). Ketamine-induced Neuroapoptosis in the Fetal and Neonatal Rhesus Macaque Brain.
580   *Anesthesiology: The Journal of the American Society of Anesthesiologists*, *116*(2), 372–384.
581   https://doi.org/10.1097/ALN.0b013e318242b2cd

582 Burkard, R. F., Don, M., & Eggermont, J. J. (2006). *Auditory Evoked Potentials: Basic Principles and*
583   *Clinical Application* (1st ed.). Philadelphia: Lippincott Williams & Williams.

584 Ching, T. Y. C., Day, J., Van Buynder, P., Hou, S., Zhang, V., Seeto, M., … Flynn, C. (2014). Language
585   and speech perception of young children with bimodal fitting or bilateral cochlear implants. *Cochlear*
586   *Implants International*, *15 Suppl 1*, S43-46. https://doi.org/10.1179/1467010014Z.000000000168

587 Creeley, C., Dikranian, K., Dissen, G., Martin, L., Olney, J., & Brambrink, A. (2013). Propofol-induced
588   apoptosis of neurones and oligodendrocytes in fetal and neonatal rhesus macaque brain. *BJA:*
589   *British Journal of Anaesthesia*, *110*(suppl_1), i29–i38. https://doi.org/10.1093/bja/aet173

590 Cullington, H. E., Bele, D., Brinton, J. C., Cooper, S., Daft, M., Harding, J., … Wilson, K. (2017). United
591   Kingdom national paediatric bilateral project: Demographics and results of localization and speech
592   perception testing. *Cochlear Implants International*, *18*(1), 2–22.
593   https://doi.org/10.1080/14670100.2016.1265055

594 Elberling, C., & Wahlgreen, O. (1985). Estimation of Auditory Brainstem Response, ABR, by Means of
595   Bayesian Inference. *Scandinavian Audiology*, *14*(2), 89–96.
596   https://doi.org/10.3109/01050398509045928

597 Eysholdt, U., & Schreiner, Chr. (1982). Maximum Length Sequences - A Fast Method for Measuring Brain-
598   Stem-Evoked Responses. *International Journal of Audiology*, *21*(3), 242–250.
599   https://doi.org/10.3109/00206098209072742

600 FDA. (2017, April 27). Drug Safety and Availability - FDA Drug Safety Communication: FDA approves label
601   changes for use of general anesthetic and sedation drugs in young children [WebContent].
602   Retrieved April 22, 2018, from https://www.fda.gov/Drugs/DrugSafety/ucm554634.htm

603 François, M., Teissier, N., Barthod, G., & Nasra, Y. (2012). Sedation for children 2 to 5 years of age
604   undergoing auditory brainstem response and auditory steady state responses recordings.
605   *International Journal of Audiology*, *51*(4), 282–286. https://doi.org/10.3109/14992027.2011.601469

606 Gorga, M. P., Johnson, T. A., Kaminski, J. R., Beauchaine, K. L., Garner, C. A., & Neely, S. T. (2006).
607   Using a Combination of Click- and Tone Burst-Evoked Auditory Brain Stem Response
608   Measurements to Estimate Pure-Tone Thresholds. *Ear and Hearing*, *27*(1), 60–74.
609   https://doi.org/10.1097/01.aud.0000194511.14740.9c

610 Harrison, R. V., Gordon, K. A., & Mount, R. J. (2005). Is there a critical period for cochlear implantation in
611   congenitally deaf children? Analyses of hearing and speech perception performance after
612   implantation. *Developmental Psychobiology*, *46*(3), 252–261. https://doi.org/10.1002/dev.20052

613 Hood, L. J. (1998). *Clinical Applications of the Auditory Brainstem Response* (1st ed.). San Diego: Singular
614   Publishing.

615   Hyde, M. (2008). *Ontario Infant Hearing Program Audiologic Assessment Protocol Version 3.1*.

616   Jevtovic-Todorovic, V., Hartman, R. E., Izumi, Y., Benshoff, N. D., Dikranian, K., Zorumski, C. F., …
617   Wozniak, D. F. (2003). Early Exposure to Common Anesthetic Agents Causes Widespread
618   Neurodegeneration in the Developing Rat Brain and Persistent Learning Deficits. *Journal of*
619   *Neuroscience*, *23*(3), 876–882. https://doi.org/10.1523/JNEUROSCI.23-03-00876.2003

620   Joint Committee on Infant Hearing. (2007). Year 2007 position statement: Principles and guidelines for
621   early hearing detection and intervention. https://doi.org/10.1044/policy.PS2007-00281

622   Korczak, P., Smart, J., Delgado, R., Strobel, T. M., & Bradford, C. (2012). Auditory Steady-State
623   Responses. *Journal of the American Academy of Audiology*, *23*(3), 146–170.
624   https://doi.org/10.3766/jaaa.23.3.3

625   Liberman, M. C., Epstein, M. J., Cleveland, S. S., Wang, H., & Maison, S. F. (2016). Toward a Differential
626   Diagnosis of Hidden Hearing Loss in Humans. *PLOS ONE*, *11*(9), e0162726.
627   https://doi.org/10.1371/journal.pone.0162726

628   Luts, H., Desloovere, C., & Wouters, J. (2006). Clinical Application of Dichotic Multiple-Stimulus Auditory
629   Steady-State Responses in High-Risk Newborns and Young Children. *Audiology and Neurotology*,
630   *11*(1), 24–37. https://doi.org/10.1159/000088852

631   May-Mederake, B. (2012). Early intervention and assessment of speech and language development in
632   young children with cochlear implants. *International Journal of Pediatric Otorhinolaryngology*, *76*(7),
633   939–946. https://doi.org/10.1016/j.ijporl.2012.02.051

634   Moeller, M. P. (2000). Early Intervention and Language Development in Children Who Are Deaf and Hard
635   of Hearing. *Pediatrics*, *106*(3), e43–e43. https://doi.org/10.1542/peds.106.3.e43

636   Özdamar, Ö., & Bohórquez, J. (2006). Signal-to-noise ratio and frequency analysis of continuous loop
637   averaging deconvolution (CLAD) of overlapping evoked potentials. *The Journal of the Acoustical*
638   *Society of America*, *119*(1), 429–438. https://doi.org/10.1121/1.2133682

639   Pittman, A. L., & Stelmachowicz, P. G. (2003). Hearing loss in children and adults: Audiometric
640   configuration, asymmetry, and progression. *Ear and Hearing*, *24*(3), 198–205.
641   https://doi.org/10.1097/01.AUD.0000069226.22983.80

642   Ramos, N., Almeida, M. G., & Lewis, D. R. (2013). Correlation between frequency-specific auditory
643   brainstem responses and behavioral hearing assessment in children with hearing loss. *Revista*
644   *CEFAC*, *15*(4), 796–802. https://doi.org/10.1590/S1516-18462013000400008

645   Robles, L., & Ruggero, M. A. (2001). Mechanics of the Mammalian Cochlea. *Physiological Reviews*, *81*(3),
646   1305–1352.

647   Stapells, D. R. (2011). *Frequency-Specific ABR and ASSR Threshold Assessment in Young Infants*.
648   Retrieved from
649   http://www.phonak.com/content/dam/phonak/gc_hq/b2b/en/events/2010/Proceedings/Pho_Chap_0
650   4_Stapells_final.pdf

651   Stapells, D. R., & Oates, P. (1997). Estimation of the Pure-Tone Audiogram by the Auditory Brainstem
652   Response: A Review. *Audiology and Neurotology*, *2*(5), 257–280.
653   https://doi.org/10.1159/000259252

654 Task Force on Newborn and Infant Hearing. (1999). Newborn and Infant Hearing Loss: Detection and
655   Intervention. *Pediatrics*, *103*(2), 527–530. https://doi.org/10.1542/peds.103.2.527

656 Valderrama, J. T., Alvarez, I., Torre, A. de la, Segura, J. C., Sainz, M., & Vargas, J. L. (2012). Recording of
657   auditory brainstem response at high stimulation rates using randomized stimulation and averaging.
658   *The Journal of the Acoustical Society of America*, *132*(6), 3856–3865.
659   https://doi.org/10.1121/1.4764511

660 Valderrama, J. T., de la Torre, A., Alvarez, I. M., Segura, J. C., Thornton, A. R. D., Sainz, M., & Vargas, J.
661   L. (2014). Auditory brainstem and middle latency responses recorded at fast rates with randomized
662   stimulation. *The Journal of the Acoustical Society of America*, *136*(6), 3233–3248.
663   https://doi.org/10.1121/1.4900832

664 Vohr, B. (2003). Overview: Infants and children with hearing loss—part I. *Mental Retardation and
665   Developmental Disabilities Research Reviews*, *9*(2), 62–64. https://doi.org/10.1002/mrdd.10070

666 Wagner, M., Ryu, Y. K., Smith, S. C., & Mintz, C. D. (2014). Review: Effects of Anesthetics on Brain Circuit
667   Formation. *Journal of Neurosurgical Anesthesiology*, *26*(4), 358–362.
668   https://doi.org/10.1097/ANA.0000000000000118

669 Wang, T., Zhan, C., Yan, G., Bohórquez, J., & Özdamar, Ö. (2013). A preliminary investigation of the
670   deconvolution of auditory evoked potentials using a session jittering paradigm. *Journal of Neural
671   Engineering*, *10*(2), 026023. https://doi.org/10.1088/1741-2560/10/2/026023

672 Wilder, R. T., Flick, R. P., Sprung, J., Katusic, S. K., Barbaresi, W. J., Mickelson, C., … Warner, D. O.
673   (2009). Early Exposure to Anesthesia and Learning Disabilities in a Population-Based Birth Cohort.
674   *Anesthesiology*, *110*(4), 796–804. https://doi.org/10.1097/01.anes.0000344728.34332.5d

675 Yoshinaga-Itano, C., Sedey, A. L., Coulter, D. K., & Mehl, A. L. (1998). Language of early- and later-
676   identified children with hearing loss. *Pediatrics*, *102*(5), 1161–1171.

677

678 **TABLES**

679

			S2	S3	S5	S6	S7	S8	S9	S10	S11	LQ	MED	UQ
75 dB peSPL	Parallel	500 Hz	0.41	4.91	1.93	3.00	22.56	0.99	0.93	0.50	3.63	0.93	1.93	3.63
		1000 Hz	0.35	0.68	0.97	0.60	2.39	0.36	0.24	0.21	1.40	0.35	0.60	0.97
		2000 Hz	0.36	0.54	0.70	0.91	1.89	0.19	0.29	0.40	0.51	0.36	0.51	0.70
		4000 Hz	0.17	0.64	0.26	0.32	1.82	0.16	0.27	0.30	0.31	0.26	0.30	0.32
		8000 Hz	0.20	0.66	0.44	0.64	2.88	0.27	0.28	0.25	0.66	0.27	0.44	0.66
		Total (MAX)	0.41	4.91	1.93	3.00	22.56	0.99	0.93	0.50	3.63	**0.93**	**1.93**	**3.63**
	Serial	500 Hz	0.18	0.73	0.61	0.27	14.24	0.35	0.15	0.09	0.79	0.18	0.35	0.73
		1000 Hz	0.06	0.19	0.27	0.06	0.77	0.12	0.05	0.07	0.22	0.06	0.12	0.22
		2000 Hz	0.07	0.19	0.16	0.13	0.79	0.08	0.07	0.05	0.14	0.07	0.13	0.16
		4000 Hz	0.05	0.32	0.15	0.10	0.74	0.08	0.06	0.08	0.21	0.08	0.10	0.21
		8000 Hz	0.11	0.41	0.43	0.16	0.66	0.09	0.08	0.11	0.36	0.11	0.16	0.41
		Total (2×SUM)	0.94	3.68	3.23	1.45	34.40	1.44	0.82	0.82	3.45	**0.94**	**1.45**	**3.45**
45 dB peSPL	Parallel	500 Hz	0.57	8.99	1.44	7.76	8.78	1.86	0.83	4.60	53.12	1.44	4.60	8.78
		1000 Hz	0.47	1.76	3.04	1.31	7.79	0.86	0.58	0.82	1.73	0.82	1.31	1.76
		2000 Hz	0.23	0.62	1.10	1.03	3.69	0.31	0.29	0.50	1.01	0.31	0.62	1.03
		4000 Hz	0.41	0.93	0.47	0.71	9.26	0.25	0.32	0.50	0.69	0.41	0.50	0.71
		8000 Hz	0.57	1.54	0.65	0.84	10.34	0.30	0.30	0.45	1.10	0.45	0.65	1.10
		Total (MAX)	0.57	8.99	3.04	7.76	10.34	1.86	0.83	4.60	53.12	**1.86**	**4.60**	**8.99**
	Serial	500 Hz	0.15	1.71	1.99	1.56	11.64	2.11	0.84	0.89	20.17	0.89	1.71	2.11
		1000 Hz	0.13	0.60	0.37	0.83	6.00	0.98	0.48	0.91	7.12	0.48	0.83	0.98
		2000 Hz	0.15	0.51	1.00	0.67	5.52	0.18	0.32	0.42	0.77	0.32	0.51	0.77
		4000 Hz	0.22	0.85	0.53	0.37	4.50	0.16	0.21	0.45	0.53	0.22	0.45	0.53
		8000 Hz	0.21	1.29	0.66	0.47	2.81	0.20	0.23	0.31	1.21	0.23	0.47	1.21
		Total (2×SUM)	1.72	9.92	9.10	7.81	60.94	7.27	4.16	5.95	59.60	**5.95**	**7.81**	**9.92**

	S2	S3	S0	S6	S7	S8	S9	S10	S11	LQ	MED	UQ
Speedup 75 dB peSPL	*2.30*	*0.75*	*1.68*	*0.48*	*1.52*	*1.45*	*0.89*	*1.64*	*0.95*	***0.89***	***1.45***	***1.64***
Speedup 45 dB peSPL	*3.00*	*1.10*	*2.99*	*1.01*	*5.90*	*3.92*	*5.03*	*1.29*	*1.12*	***1.12***	***2.99***	***3.92***

680

681 **Table 1.** Time to 0 dB SNR (in minutes) for each subject as well as the median and quantiles. For each
682 method at each stimulus level the time is shown for all frequencies, with the total (computed with the
683 appropriate method) shown below. Shown at the bottom in italics are the speedups for both stimulus levels.
684 These numbers are unitless ratios, rather than minutes, where higher numbers represent an advantage for
685 the pABR over the serial ABR.

686

687 **FIGURE CAPTIONS**

688 **Figure 1.** pABR stimulus construction. (**A**) Individual toneburst stimuli for each frequency. (**B**) Toneburst
689 trains in each ear (colored lines) are summed to create a two-channel (left, right) stimulus epoch (black
690 lines).

691

692 **Figure 2.** The distribution of inter-stimulus intervals over all stimuli for $\lambda = 40$ stimuli / s (solid gray)
693 compared to the predicted distribution given by $P(t) = 40e^{-40t}$. There is a very close match indicating that
694 the deviations from a true Poisson point process used in this experiment are negligible.

695

696 **Figure 3.** The analysis chain, shown from stimulus creation and presentation to calculation of response
697 waveforms. For clarity, only a 50 ms time period is shown. Dashed box: Zero-padding scheme shown for a
698 single impulse train of a single epoch. Note t_{pre} and t_{post} are not shown to scale.

699

700 **Figure 4.** Intensity series waveforms across frequencies and for the left and right ears. (**A**) Grand average
701 of 8 subjects. (**B**,**C**) Two example subjects' responses. All responses are plotted over the interval 0 to 25
702 ms.

703

704 **Figure 5.** Mean wave V latency (**A**) and amplitude (**B**) as a function of intensity. Stimulus frequency is
705 indicated on each line. Error bars (where large enough to be seen) indicate ±1 SEM. Lines have a slight
706 horizontal offset in **B** to reduce overlap.

707

708 **Figure 6.** Parallel vs series acquisition waveforms (right ear only). (**A**) Grand average. (**B**,**C**) Example
709 subjects. pABR is shown in colored lines. Corresponding serial waveforms are shown in black. Vertical
710 spacing is 0.3 µV / div.

711

712 **Figure 7.** Comparison of pABR with serial wave V latency (**A**) and amplitude (**B**) for all subjects (N = 9) at
713 each frequency for both stimulus levels. Quantities shown are for the right ear. Stimulus frequency
714 indicated by marker number and color.

715

716 **Figure 8.** Comparison of time to reach 20 nV residual noise for all 10 waveforms between methods (pABR
717 in black, serial in gray). Two intensities for 9 subjects are shown, leading to 18 data points for each
718 acquisition method.

719

720 **Figure 9.** pABR shows faster acquisition and better SNR. (**A**) Real-time acquisition runs simulated from
721 offline data for one subject at 45 dB peSPL. For serial ABR, unrecorded left ear runs were assumed to be
722 equal to right ear. (**B**) Comparison recording time for 9 subjects. Points below dotted unity line are cases
723 where pABR is faster. Shaded regions indicate speedup ratios of 1–2 (light gray), 2–4 (medium gray), and
724 > 4 (dark gray). (**C**) SNR of pABR runs upon serial acquisition completion (subjects colored points, median
725 black lines), corresponding for one subject to the points on the red dashed vertical line in **A**.

726

727 **Figure 10.** Improved visual response detection. (**A**) 500 Hz response waveform alone. (**B**) Same response
728 with other frequencies simultaneously acquired. Dotted gray box surrounds the waveform from **A**. (**C**) 500
729 Hz response with other frequencies present and analysis window extended 10 ms to the left and 20 ms to
730 the right. Gray box as in **B**.

731

732 **Figure 11.** Parallel stimulation allows toneburst trains to also function as notched noise. (**A**) Cartoon
733 representation of a single toneburst stimulus in the frequency domain (filled area), and the pattern of
734 excitation it evokes in the cochlea (dashed line), showing spread of excitation towards the basal end. (**B**)
735 Notched noise can be used to mask the off-frequency excitation, yielding a more place-specific response.
736 (**C**) In pABR, each frequency band is masked by the others, which summed have a similar effect to a
737 notched noise masker.